Structure and ion-dependent folding of k-junctions

Mengxiao Li, Jie Deng, Xuemei Peng, Jia Wang, Timothy J. Wilson, Lin Huang, David M. J. Lilley

SUPPLEMENTARY INFORMATION

SUPPLEMENTARY FIGURES

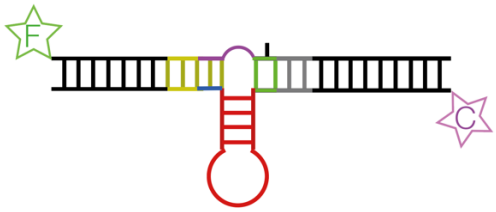

Arabidopsis TPP riboswitch k-junction
F- CCAGUCAGCCCU UU GAACCCAUGUCAGG
GGUCAGUCGGGA CCAG AAAG CUGG A GGGGUACAGUCC-Cy3

E. coli TPP riboswitch k-junction
F-CCAGUCAGCCCG U AUCACCCAUGUCAGG
GGUCAGUCGGGC UCAG AAAG CUGA A GGGGUACAGUCC-Cy3

DUF2368 k-junction
F-CCAGUCAGGAGU UA GACUCAUGUCAGG
GGUCAGUCUUCA UGAC AAAG GUCA AGGAGUACAGUCC-Cy3

Supplementary Figure 1. Full sequences of k-junctions used in analysis of folding by steady-state FRET. The C and NC arms were extended to a total of 12 and 13 bp respectively (including the G:A sheared base pairs and the interactions made by the connecting dinucleotide). Fluorescein (F) and cyanine-3 (Cy3) were attached to the 5′ termini of the *b* (top as shown) and *n* (lower) strand. For each construct the top strand is written 5′ to 3′ and the lower strand 3′ to 5′.

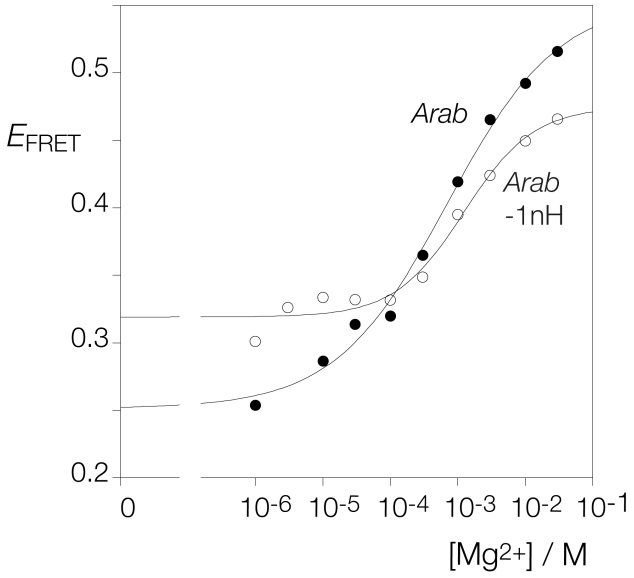

Supplementary Figure 2. Effect of -1nH variation on Mg^{2+} ion induced folding of the *Arabidopsis* TPP riboswitch k-junction. FRET efficiency (E_{FRET}) plotted as a function of Mg^{2+} ion concentration and fitted to a simple two-state binding model (lines). *Filled circles* : natural sequence *Arabidopsis* k-junction. *Open circles* : *Arabidopsis* k-junction with -1n O2'H substitution.

5' GGGAGUUAGACUCGCGAAAGCGAGGAACUGCGAAAGCAGUACUUCC 3'

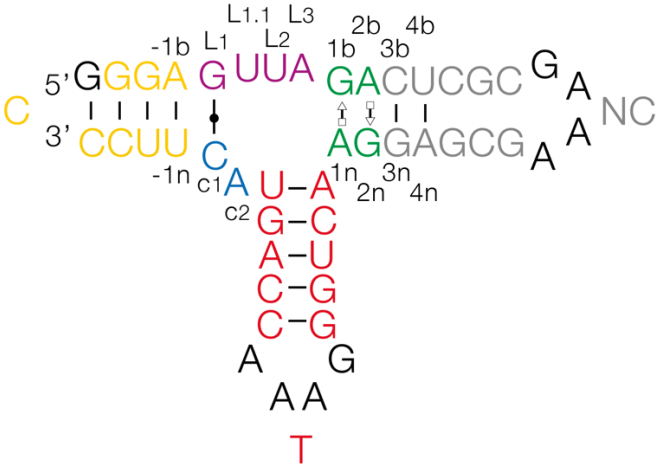

Supplementary Figure 3. Sequence of the DUF-3268 k-junction used for X-ray crystallography.

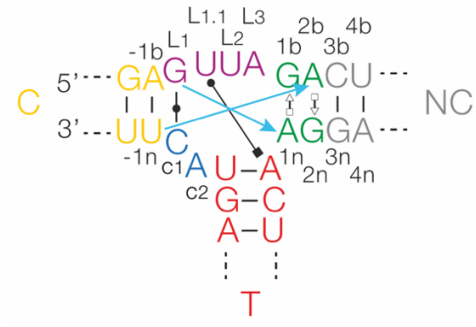

functional position	PDB
G 1b	9
A 2b	10
A 1n	26
G 2n	25
G L1	5
U L1.1	6
U L2	7
A L3	8
A -1b	4
U -1n	43
A c2	41
C c1	42

Supplementary Figure 4. The correspondence between the standard nomenclature for nucleotide positions in the k-junction with the numbering in the PDB file of the crystal structure of DUF-3268.

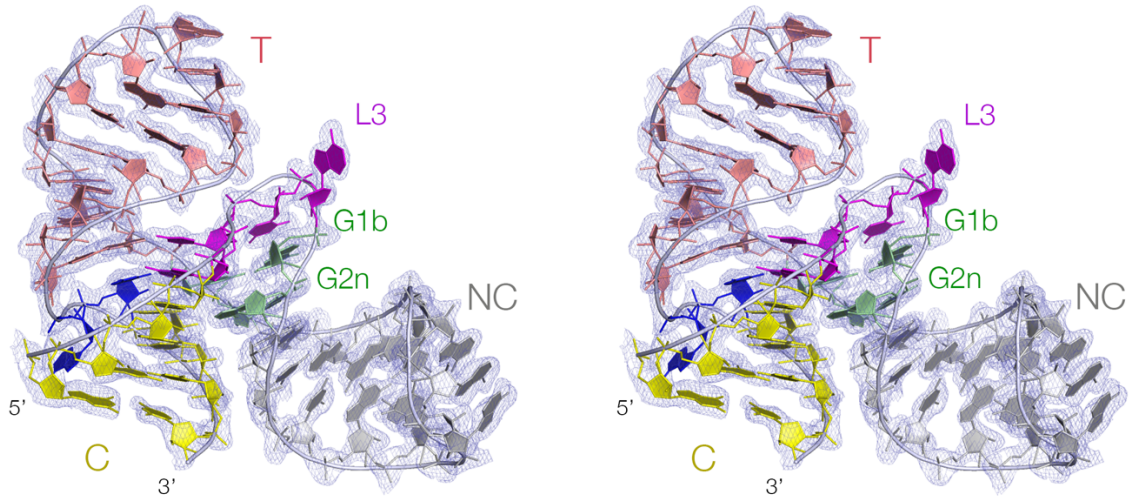

Supplementary Figure 5. Structure of the complete DUF-3268 k-junction structure in the crystal. The structure is shown as a parallel-eye stereoscopic view, with the F_o-F_c electron density map contoured at 1 σ. The view shown is onto the minor groove side of the L1-L3 loop.

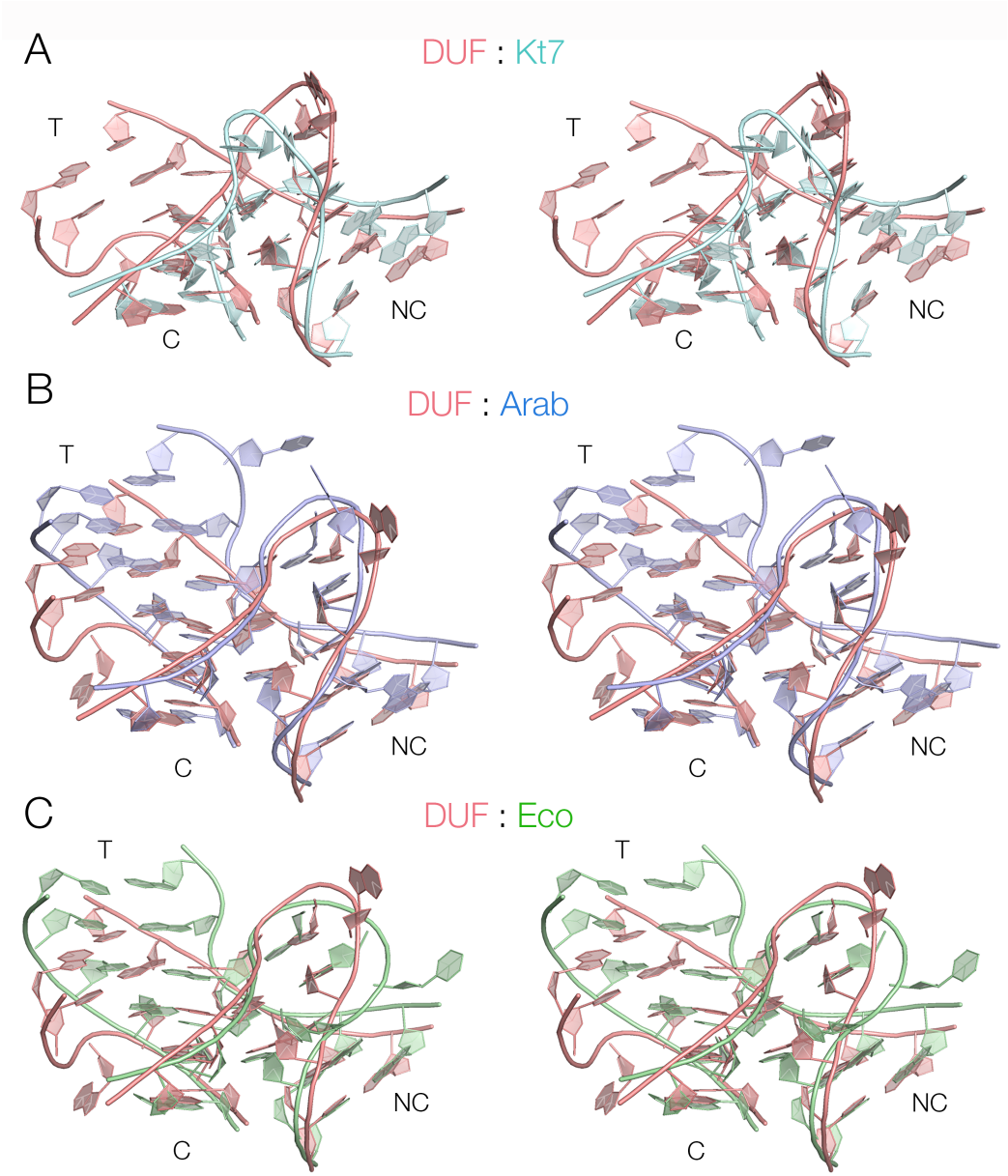

Supplementary Figure 6. Superposition of the DUF-3268 k-junction structure with other k-junctions and a standard k-turn. The DUF-3268 k-junction (red) is superimposed with **A**. the *H. marismortui* Kt-7 k-turn (cyan), **B**. the *Arabidopsis* k-junction (blue) and **C**. the *E. coli* k-junction (green). The root-mean square values for the pairings are :

DUF k-junction *vs* Kt7 k-turn = 1.68 Å (64 to 64 atoms)

DUF k-junction *vs* *Arab* k-junction = 1.58 Å (64 to 64 atoms)

DUF k-junction *vs* *Eco* k-junction = 2.13 Å (64 to 64 atoms)

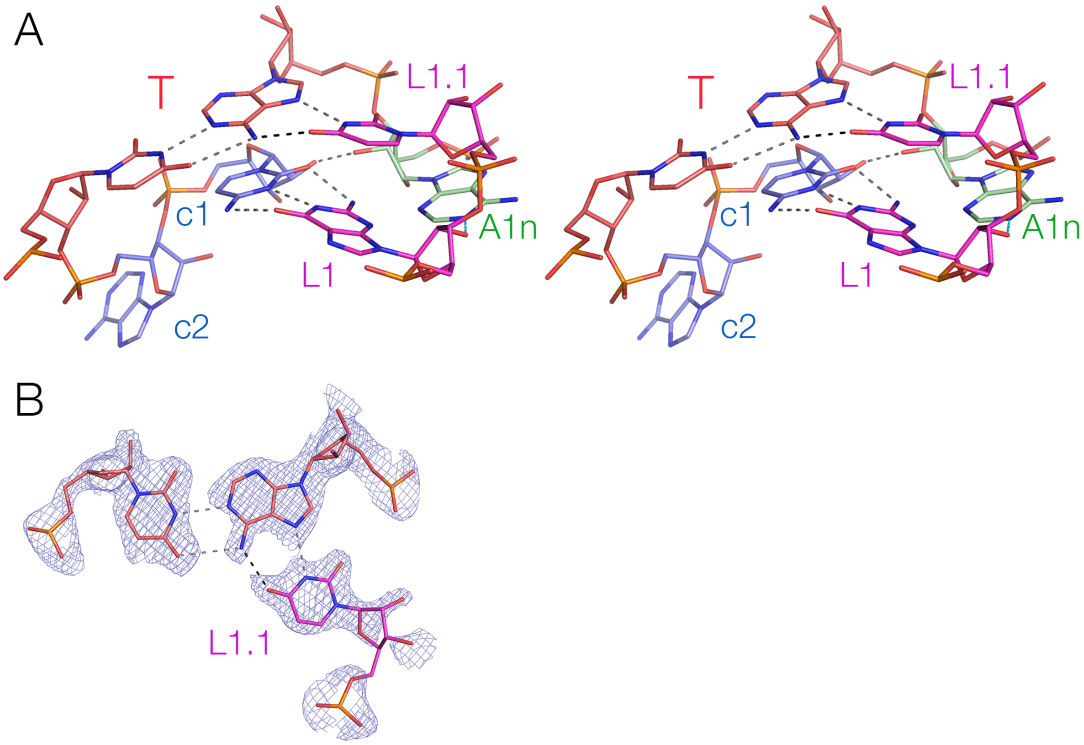

Supplementary Figure 7. L1 and L1.1 interactions in the crystal structure of the DUF-3268 k-junction. **A**. Parallel-eye stereoscopic view of the in-plane interactions of L1 with c1 (standard *cis* Watson-Crick base pair) and L1.1 with the Hoogsteen edge of the adenine of the junction-proximal base pair of the T helix. **B**. The L1.1 triple base interaction, with the F_o-F_c electron density map contoured at 1 σ.

E. coli TPP riboswitch
GGACUCGGGGUGCCCUUCUGCGUGAAGGCUGAGAAAUACCCGUAUCACCUGAUCUGGA
UAAUGCCAGCGUAGGGAAGUUC

DUF chimeric TPP riboswitch
GGAGUACUUGUGCCCUUCUGCGUGAAGGCUGAGAAAUAGAGUUAGACUUGAUCUGGAUA
AUGCCAGCGUAAGGAACUUC

DUF A1nU chimeric TPP riboswitch
GGAGUACUUGUGCCCUUCUGCGUGAAGGCUGAGAAAUAGAGUUAGACUUGAUCUGGAUA
AUGCCAGCGUAAGGUACUUC

Supplementary Figure 8. *E. coli* and DUF-3268 chimeric TPP riboswitches used in gel electrophoretic and calorimetric analysis. The A1nU mutation is highlighted yellow. All sequences written 5′ to 3′.

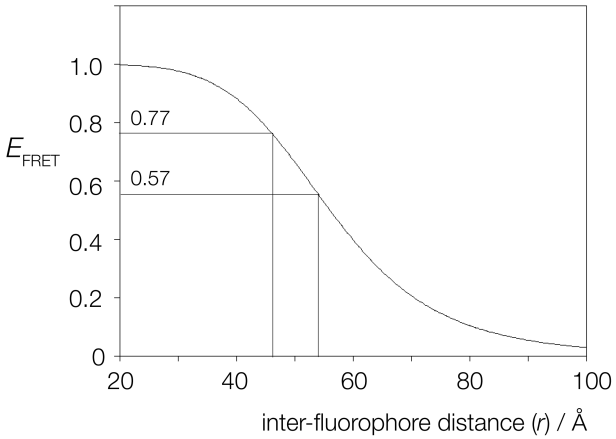

Supplementary Figure 9. The dependence of FRET efficiency (E_{FRET}) upon separation of fluorophores (r) for R_0 = 56 Å i.e. the value for fluorescein-cyanine 3. This was computed using equation (1). The positions corresponding to the measured maximum E_{FRET} for the *Arabidopsis* (0.57) and DUF-3268 (0.77) k-junctions are marked.

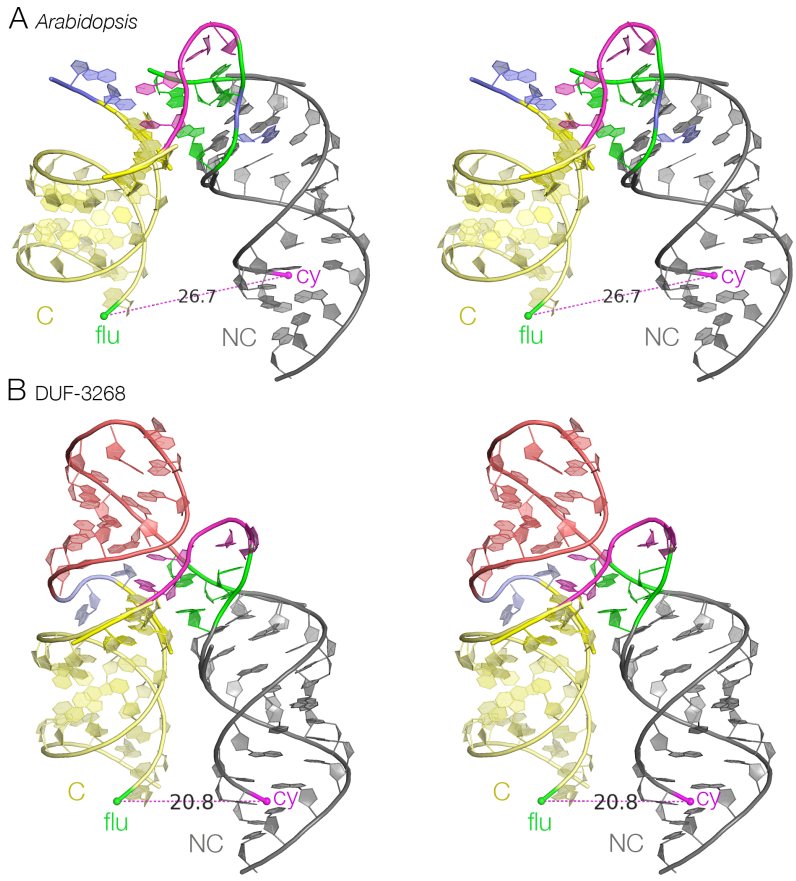

Supplementary Figure 10. The structures of the *Arabidopsis* (**A**) and DUF-3268 (**B**) k-junctions with C and NC helices extended by A-form helical RNA to model the forms used for FRET analysis, shown as parallel-eye stereoscopic views. The phosphate groups to which the fluorophores are attached in these studies are marked green (flu – fluorescein donor) and magenta (cy – cyanine 3 acceptor) are marked. The distances between the two phosphate groups are indicated for each structure.

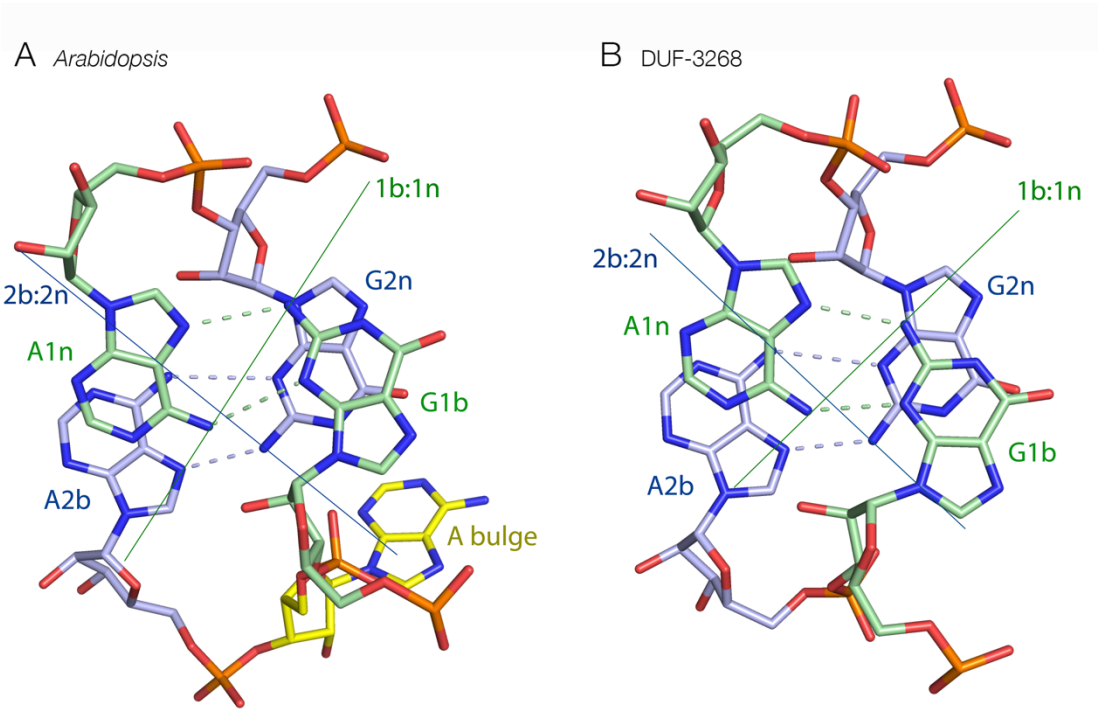

Supplementary Figure 11. Helical rotation between the G1b:A1n and A2b:G2n base pairs of the *Arabidopsis* (**A**) and DUF-3268 (**B**) k-junctions. These are viewed down the helical axis of the NC helix. For clarity the 1b:1n base pairs are colored green and the 2b:2n base pairs are blue. The bulged A of the *Arabidopsis* k-junction is colored yellow. Lines are drawn connecting the A N6 and G N2 for each G:A base pair. The angle subtended for the *Arabidopsis* and DUF-3268 k-junctions are 97° and 87° respectively. Thus there is a difference in helical rotation of 10° between the two k-junctions.

SUPPLEMENTARY TABLES

Name	k-junction
PDB	8ITS
Data collection	
Space group	C 1 2 1
Cell dimensions	
a, *b*, *c* (Å)	79.54, 38.73, 49.80
α, *β*, *γ* (°)	90 125.83 90
Wavelength	0.97851
Resolution (Å)	20.19 - 1.94 (1.99 - 1.94)
R_{merge}	0.123 (0.724)
R_{pim}	0.080 (0.626)
$I / \sigma I$	7.9 (1.5)
CC (1/2)	0.994 (0.536)
Completeness (%)	96.2 (74.0)
Redundancy	5.8 (3.5)
Refinement	
Resolution (Å)	20.19 - 1.94 (2.01 - 1.94)
No. reflections	8881 (690)
R_{work} / R_{free}	0.202 / 0.220 (0.295 / 0.400)
No. atoms	
macromolecules	993
ligands	3
solvent	118
B-factors	
macromolecules	30.33
ligands	31.15
solvent	
R.m.s. deviations	
Bond lengths (Å)	0.001
Bond angles (°)	0.33

*Values in parentheses are for highest-resolution shell.

Supplementary Table 1. Details of data collection and refinement statistics for the crystallographic data for the DUF-3268 k-junction as deposited with the PDB with ID 8ITS.

k-junction	*n*	ΔH / kJ mol^{-1}	-TΔS / kJ mol^{-1}	ΔG / kJ mol^{-1}	K_d / M
*Eco*WT 1	0.875 ± 1.8e-3	-52.5 ± 0.352	7.60	-44.9	13.7e-9 ± 1.92e-9
*Eco*WT 2	0.957 ± 2.2e-3	-53.5 ± 0.418	10.1	-43.4	25.7e-9 ± 3.16e-9
*Eco*WT 3	0.920 ± 1.3e-3	-56.4 ± 0.274	13.6	-42.8	32.3e-9 ± 2.65e-9
DUF 1	0.485 ± 4.6e-3	-43.6 ± 0.738	5.37	-38.2	206e-9 ± 32.4e-9
DUF 2	0.492 ± 2.2e-3	-45.7 ± 0.362	7.93	-37.7	249e-9 ± 17.1e-9
DUF 3	0.467 ± 2.2e-3	-44.6 ± 0.371	7.24	-37.4	289e-9 ± 19.5e-9
DUF A1nU 1	no binding				
DUF A1nU 2	no binding				
DUF A1nU 3	no binding				

Supplementary Table 2. Thermodynamic data for TPP binding to the *E. coli* TPP riboswitch and variants obtained from ITC experiments. The experiments were based on the *E. coli* TPP riboswitch and two variants, each performed in triplicate. These species are :

*Eco*WT 1-3 : Wild type *E. coli* TPP riboswitch

DUF 1-3 : Chimeric *E.coli* TPP riboswitch in which the k-junction was replaced with that from DUF-3268

DUF A1nU 1-3 : Chimeric TPP riboswitch where the DUF k-junction has an A1nU mutation

TPP was titrated into a 30 μM solution of RNA in 40 mM Hepes (pH 7.5), 100 mM KCl, 10 mM $MgCl_2$ at 25°C.